

Fluorescence and Bioluminescence Imaging of Angiogenesis in Flk1-Nano-lantern Transgenic Mice

著者	Matsushita Jun, Inagaki Shigenori, Nishie Tomomi, Sakasai Tomoki, Tanaka Junko, Watanabe Chisato, Mizutani Ken-ichi, Miwa Yoshihiro, Matsumoto Ken, Takara Kazuhiro, Naito Hisamichi, Kidoya Hiroyasu, Takakura Nobuyuki, Nagai Takeharu, Takahashi Satoru, Ema Masatsugu
journal or publication title	Scientific reports
volume	7
page range	46597
year	2017-04
権利	(C) The Author(s) 2017 This work is licensed under a Creative Commons Attribution 4.0 International License. The images or other third party material in this article are included in the article's Creative Commons license, unless indicated otherwise in the credit line; if the material is not included under the Creative Commons license, users will need to obtain permission from the license holder to reproduce the material. To view a copy of this license, visit http://creativecommons.org/licenses/by/4.0/
URL	http://hdl.handle.net/2241/00146281

doi: 10.1038/srep46597

SCIENTIFIC REPORTS



OPEN

Fluorescence and Bioluminescence Imaging of Angiogenesis in *Flk1-Nano-lantern* Transgenic Mice

Jun Matsushita^{1,*}, Shigenori Inagaki^{2,*}, Tomomi Nishie¹, Tomoki Sakasai³, Junko Tanaka³, Chisato Watanabe⁴, Ken-ichi Mizutani⁴, Yoshihiro Miwa³, Ken Matsumoto¹, Kazuhiro Takara⁵, Hisamichi Naito⁵, Hiroyasu Kidoya⁵, Nobuyuki Takakura⁵, Takeharu Nagai², Satoru Takahashi^{6,7,8} & Masatsugu Ema^{1,9}

Received: 18 April 2016
Accepted: 22 March 2017
Published: 20 April 2017

Angiogenesis is important for normal development as well as for tumour growth. However, the molecular and cellular mechanisms underlying angiogenesis are not fully understood, partly because of the lack of a good animal model for imaging. Here, we report the generation of a novel transgenic (Tg) mouse that expresses a bioluminescent reporter protein, *Nano-lantern*, under the control of *Fetal liver kinase 1 (Flk1)*. *Flk1-Nano-lantern* BAC Tg mice recapitulated endogenous *Flk1* expression in endothelial cells and lymphatic endothelial cells during development and tumour growth. Importantly, bioluminescence imaging of endothelial cells from the aortic rings of *Flk1-Nano-lantern* BAC Tg mice enabled us to observe endothelial sprouting for 18 hr without any detectable phototoxicity. Furthermore, *Flk1-Nano-lantern* BAC Tg mice achieved time-lapse luminescence imaging of tumour angiogenesis in freely moving mice with implanted tumours. Thus, this transgenic mouse line contributes a unique model to study angiogenesis within both physiological and pathological contexts.

The formation of new blood vessels, termed angiogenesis, is important for embryonic development. The basic steps of angiogenesis include degradation of the extracellular matrix, directed migration of endothelial cells (ECs), EC proliferation, EC tube formation, vessel maturation and stabilization by the recruitment of mural cells, and the deposition of the extracellular matrix. During this process, ECs adopt two distinct cellular types, tip and stalk cells. Endothelial tip cells spearhead new sprouts with dynamic filopodia and determine the direction of migration. Following tip cells, stalk cells extend fewer filopodia and support sprout elongation with their highly proliferative ability¹. Tip cells anastomose with cells from neighbouring sprouts and form the vascular lumen. Phalanx cells align in a smooth cobblestone monolayer that has tight junctions and contact with mural cells².

A blood vessel network is crucial for tumour progression³. Therefore, angiogenesis in tumours is considered to be one of the most important therapeutic targets^{4,5}. Blood vessels in tumours are highly irregular compared with those in normal organs. Unlike normal vessels, tumour vessels are dilated and tortuous with leaky saccular shapes^{6,7}. An abnormal endothelial layer is also observed in tumours. Tumour vessels are poorly interconnected with overlapping cells and shunting that compromises blood flow. In addition, it is difficult to distinguish between arteries and veins. These specific phenotypes of tumour vessels lead to poor drug delivery^{8,9}. Phalanx cells arise in

¹Department of Stem Cells and Human Disease Models, Research Center for Animal Life Science, Shiga University of Medical Sciences, Seta, Tsukinowa-cho, Otsu, Shiga 520-2192, Japan. ²Graduate School of Frontier Biosciences, Osaka University, 1-3 Yamadaoka, Suita, Osaka 565-0871, Japan. ³Department of Molecular Pharmacology, Faculty of Medicine, University of Tsukuba, Tsukuba 305-8575, Ibaraki, Japan. ⁴Laboratory of Neural Differentiation, Graduate School of Brain Science, Doshisha University, 1-3 Tatara Miyakodani, Kyotanabe-shi, Kyoto 610-0394, Japan. ⁵Department of Signal Transduction, Research Institute for Microbial Diseases, Osaka University, 3-1 Yamadaoka, Suita, Osaka 565-0871, Japan. ⁶Department of Anatomy and Embryology, Faculty of Medicine, University of Tsukuba, Tennodai 1-1-1, Tsukuba, Ibaraki 305-8577, Japan. ⁷Center for Tsukuba Advanced Research Alliance, University of Tsukuba, 1-1-1 Tennodai, Tsukuba, Ibaraki 305-8577, Japan. ⁸International Institute for Integrative Sleep Medicine, Life Science Center, and Laboratory Animal Resource Center, University of Tsukuba, 1-1-1 Tennodai, Tsukuba, Ibaraki 305-8577, Japan. ⁹Precursory Research for Embryonic Science and Technology, Japan Science and Technology Agency, 4-1-8 Honcho Kawaguchi, Saitama 332-0012, Japan. *These authors contributed equally to this work. Correspondence and requests for materials should be addressed to M.E. (email: mema@belle.shiga-med.ac.jp)

heterozygous *Phd2*-deficient ECs, leading to improvement in treatment with chemotherapy¹⁰. Tip cells promote the outgrowth of tumour cells in metastatic regions but not the outgrowth of stalk cells¹¹.

In the embryo, vascular endothelial growth factor (VEGF)-A is a key factor that regulates angiogenesis¹². VEGF-A interacts with two receptors, Flt1 and Flk1. Flk1 is known as the primary receptor that regulates most of the endothelial responses such as the proliferation and migration of ECs, vascular permeability, and the selection of tip and stalk cells. Flt1 functions as a decoy receptor because of its weak tyrosine kinase activity¹³. *Flk1* is highly expressed in tip cells. Conversely, *Flt1* expression is more prominent in stalk cells. Furthermore, the morphology of tip and stalk cells is determined by Flk1 signalling¹⁴.

In tumours, VEGF-A is considered to be one of the most important therapeutic targets. Although recent clinical studies of tumours have indicated that VEGF-A agents show promising benefits, largely negative results have been obtained^{15–17} due to the resistance to Bevacizumab¹⁸. Therefore, we need to understand the precise molecular mechanisms of VEGF-A/Flk1 signalling during tumour progression.

Because green fluorescent protein (GFP) emits strong and clear green fluorescence, it has been used to monitor gene expression in many studies. However, the fluorescence requires excitation by light that often causes phototoxicity and difficulty in distinguishing GFP fluorescence from the autofluorescence of mammalian tissues. Recently, a chimeric gene encoding the bright fluorescent protein Venus and an enhanced version of Renilla luciferase, called *Nano-lantern*, was developed to overcome these issues¹⁹. *Nano-lantern* protein emits bioluminescence without light excitation¹⁹.

Here, we report the generation of a novel transgenic (Tg) mouse that expresses *Nano-lantern* under the control of *Flk1*. *Flk1-Nano-lantern* BAC Tg mice recapitulate endogenous *Flk1* expression including its expression in the dorsal aorta and micro blood vessels during development and tumour growth. Importantly, bioluminescence imaging of ECs from the aortic rings of *Flk1-Nano-lantern* BAC Tg mice enabled us to observe endothelial sprouting without phototoxicity. Furthermore, *Flk1-Nano-lantern* BAC Tg mice achieved video-rate luminescence imaging of tumour angiogenesis in freely moving mice with implanted tumours. Thus, the EC-specific reporter line will be useful for studying normal and pathological angiogenesis.

Results

Generation of *Flk1-Nano-lantern* BAC transgenic mice. Previously, we generated *Flk1-GFP* BAC Tg mice that are useful for monitoring *Flk1* gene activity during development and in adults^{20,21}. However, when *Flk1-GFP* BAC Tg mice were used for live imaging of ECs²², the ECs that sprouted from an aortic ring of adults underwent apoptosis gradually because of phototoxicity, so the model was unsuitable for long-term (>6 hr) live imaging (K. M. unpublished observation). Recently, the *Nano-lantern* bioluminescent protein was developed so that Venus luminesces in yellowish-green light when luciferase catalyses a substrate such as coelenterazine-h¹⁹, achieving live imaging without phototoxicity. Therefore, *Nano-lantern* was introduced into the *Flk1* BAC clone (Fig. 1A) and the resulting *Nano-lantern*-carrying BAC was injected into pronuclei to create *Flk1-Nano-lantern* BAC Tg mice. Five of the eight lines showed clear Venus fluorescence in the adult ears. *Flk1-Nano-lantern* BAC Tg mice were genotyped routinely by inspection of Venus fluorescence in neonatal skin or the adult ear (Fig. 1B, Supplementary Fig. 1A). When embryonic expression of Venus in *Flk1-Nano-lantern* BAC Tg mice was analysed, Venus expression was localized in blood vessels including the dorsal aortae and the vascular plexus of the yolk sac (Fig. 1C).

Expression of Venus from *Flk1-Nano-lantern* during development. To examine whether *Flk1-Nano-lantern* BAC Tg mice are useful for fluorescence imaging, we compared the fluorescent intensity of Venus in ECs of *Flk1-Nano-lantern* BAC Tg mice with that of *Flk1+/GFP* knock-in mice²³ because *Flk1+/GFP* knock-in mice have been used to monitor endogenous *Flk1* protein and in other experiments^{23–25} including live imaging²⁴. The fluorescence intensity of Venus in the blood vessels of *Flk1-Nano-lantern* BAC Tg mice at embryonic day (E) 9.5 was comparable with that of *Flk1+/GFP* knock-in mice (Fig. 1D, Supplementary Fig. 1B). Higher magnification of *Flk1-Nano-lantern* BAC Tg embryos revealed Venus fluorescence in blood vessels at a comparable level as that in *Flk1+/GFP* knock-in mice (Fig. 1E and E', Supplementary Fig. 1C). To compare Venus expression with endogenous *Flk1* protein expression, we performed immunohistochemistry at E9.5 and found that Venus expression overlapped well with *Flk1* protein expression in ECs including in the dorsal aorta, vitelline vein and micro capillaries (Fig. 2, Supplementary Fig. 2). Furthermore, immunohistochemistry on tissue sections confirmed the overlapping expression of endogenous *Flk1* and Venus (Fig. 3A). Flow cytometric analysis of E9.5 foetuses also clearly indicated the expression of Venus in ECs of *Flk1-Nano-lantern* BAC Tg mice, which overlapped with endogenous *Flk1* at the cellular level and was consistent with that in *Flk1+/GFP* knock-in mice (Fig. 3B).

Previous studies demonstrate the expression of *Flk1* in lymphatic ECs, which has important functions during lymphangiogenesis²⁶. To examine Venus expression in lymphatic vessels, the back skin of a *Flk1-Nano-lantern* BAC Tg foetus at E13.5 was removed and subjected to immunohistochemistry for lymphatic vessel markers, Prox1 (Prospero homeobox 1) and LYVE-1 (lymphatic vessel endothelial hyaluronan receptor 1). We found that Prox1 and LYVE-1-positive lymphatic ECs integrated into tubular structures were positive for Venus, indicating that Venus expression driven by *Flk1-Nano-lantern* BAC recapitulates the endogenous expression of *Flk1* in lymphatic ECs (Fig. 4, Supplementary Fig. 3). We also examined Venus expression in various organs of *Flk1-Nano-lantern* BAC Tg mice at E13.5. Overall, most organs from *Flk1-Nano-lantern* BAC Tg mice exhibited a similar intensity and pattern of luminescence as those in *Flk1+/GFP* knock-in mice (Fig. 5).

Luminescence imaging of ECs in aortic rings from *Flk1-Nano-lantern* BAC Tg mice. The aortic ring assay is the standard method to evaluate angiogenesis *in vitro* by measuring the number and length of sprouting blood vessels from an aortic ring²⁷. Aortic rings were isolated from *Flk1-Nano-lantern* BAC Tg mice and *Flk1+/GFP* mice and were cultured in the presence of VEGF-A for 1 week so that the aortic rings extended

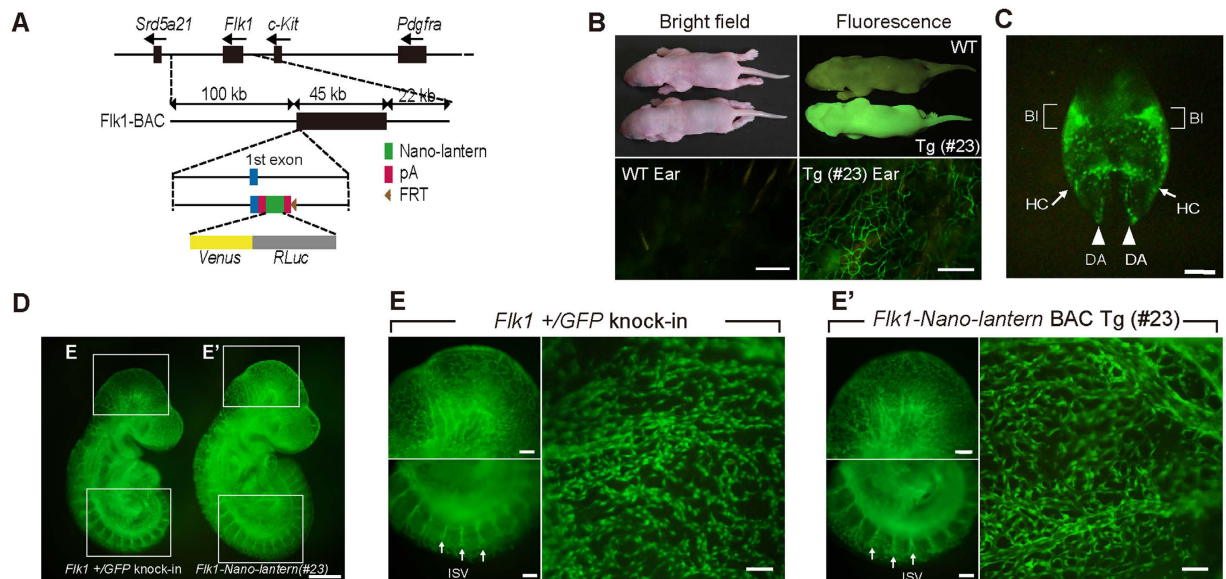


Figure 1. Generation of *Flk1*-Nano-lantern BAC Tg mice. (A) Schematic representation of the *Flk1*-Nano-lantern BAC transgene used in this study. The *Flk1* BAC clone (RP24-125B24) was used to drive *Nano-lantern*, a chimeric gene encoding the bright fluorescent protein Venus and an enhanced version of Renilla luciferase (RLuc). (B) Gross appearance of *Flk1*-Nano-lantern BAC Tg mice. Bright field and Venus fluorescence images (top panel) of newborns and an adult ear are shown. (C) Venus expression in the blood vessels of an 8.5 dpc embryo. DA: dorsal aorta; BI: blood island; HC: heart crescent. (D) Fluorescence intensity in an *Flk1*+/*GFP* knock-in embryo and an *Flk1*-Nano-lantern BAC Tg embryo (#23). (E) (E') Venus expression in the blood vessels of a 9.5 dpc *Flk1*+/*GFP* knock-in embryo (E) and *Flk1*-Nano-lantern BAC Tg embryo (#23) (E'). Arrows indicate ISV. ISV: intersomitic vessel. Scale bars: 100 m (B), 300 m (C), 500 m (D), and 200 m (E).

sprouts in a VEGF-dependent manner. Immunohistochemistry with anti-GFP and anti-Flk1 antibodies clearly showed that the ECs that sprouted from the aortic rings of *Flk1*-Nano-lantern BAC Tg mice exhibited a similar level and pattern of fluorescence as GFP in *Flk1*+/*GFP* knock-in mice (Supplementary Fig. 4). This result demonstrated that *Flk1*-Nano-lantern BAC Tg animals are useful for visualizing *Flk1*-expressing ECs *in vitro*. However, the fluorescence requires excitation by light that often causes phototoxicity and difficulty in distinguishing GFP fluorescence from the autofluorescence of mammalian tissues. In fact, *Flk1*-GFP BAC Tg mice were unsuitable for long-term (>6 hr) live imaging due to phototoxicity (K. M. unpublished observation). When the aortic rings from *Flk1*-Nano-lantern BAC Tg mice were subjected to bioluminescence imaging according to Saito *et al.*¹⁹, a bright bioluminescence was detected (Fig. 6A). Furthermore, by capturing the luminescence every 30 min over a period of 18 hr, the observation of EC sprouting was achieved without phototoxicity (Fig. 6B, Supplementary Movie S1), showing a clear advantage over *Flk1*-GFP BAC Tg mice.

Bioluminescence imaging of tumour blood vessels in *Flk1*-Nano-lantern BAC Tg mice. *Flk1* is expressed abundantly in the ECs of developing embryos but decreases to a low level in adult tissues^{28,29}. However, it is re-activated in the neovasculature associated with tumour formation³⁰. Accordingly, RT-qPCR analysis showed that *Flk1* mRNA was expressed abundantly in ECs from embryos at E8.5 and down-regulated in CD31-positive/CD45-negative ECs isolated from adult skin (Fig. 7A). Further RT-qPCR analysis showed that *Flk1* mRNA was up-regulated by three-fold in CD31-positive/CD45-negative ECs of LLC tumours 8 days after implantation (Fig. 7A). Consistent with the RT-qPCR data, immunohistochemical analysis with anti-Flk1 antibody clearly demonstrated that Venus and Flk1 expressions are well-overlapped in the tumour endothelial cells (Fig. 7B).

To detect bioluminescence from *Flk1*-Nano-lantern BAC Tg mice with a C57BL/6 background, the mice were back-crossed to the C57BL/6 albino (B6 (Cg)-Tyr^{c-2J}) strain (Fig. 8A). LLC cells were implanted into the backs of *Flk1*-Nano-lantern BAC Tg mice at two different time points, and *Flk1*-Nano-lantern BAC Tg mice showed two tumours of different sizes from the cells implanted 8 days and 11 days before (Fig. 8B). When coelenterazine-h was administered into the tumour as described in Materials and Methods, we detected a rapid up-regulation of bioluminescence in the tumours of *Flk1*-Nano-lantern BAC Tg mice (Fig. 8B), but no detectable background in WT mice. The intensity of the bioluminescence in the tumour on day 11 was stronger than that on day 8 (Fig. 8C). Furthermore, owing to the intense bioluminescence, we were able to observe luminescence from the tumour ECs in freely moving mice at a video-rate (Fig. 8C). Taken together, these results demonstrated that *Flk1*-Nano-lantern BAC Tg mice are a valuable transgenic animal for the non-invasive detection of pathological angiogenesis, such as tumour angiogenesis, in live mice.

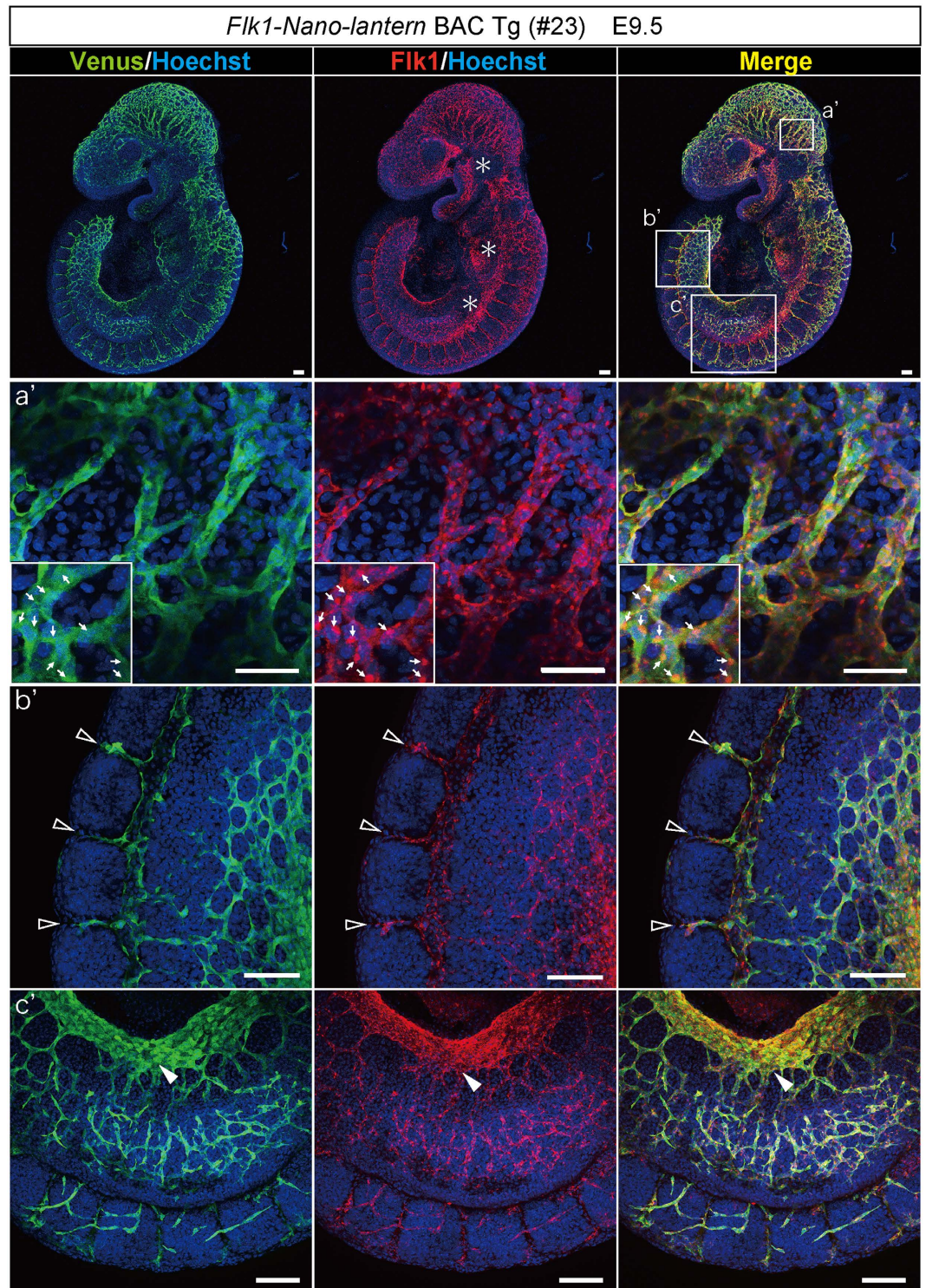


Figure 2. Co-expression of endogenous *Flk1* and *Nano-lantern* driven by the *Flk1* regulatory sequence in vascular ECs. Co-expression of Venus and the endogenous *Flk1* protein in *Flk1-Nano-lantern* BAC Tg embryos at 9.5 dpc. Tg embryos were subjected to immunohistochemical analysis with anti-GFP and anti-*Flk1* antibodies. *Indicates strong autofluorescence caused by circulating blood cells. Circulating blood cells localized in blood vessels are also shown by arrows. Open arrowheads and a closed arrowhead indicate intersomitic vessels and the vitelline vein, respectively. Scale bars: 100 μ m.

Discussion

Similar to *Flk1*+/*GFP* knock-in mice, we have shown that the *Flk1-Nano-lantern* BAC Tg mice generated in this study recapitulate endogenous *Flk1* expression in blood vessels during development. *Flk1-Nano-lantern*

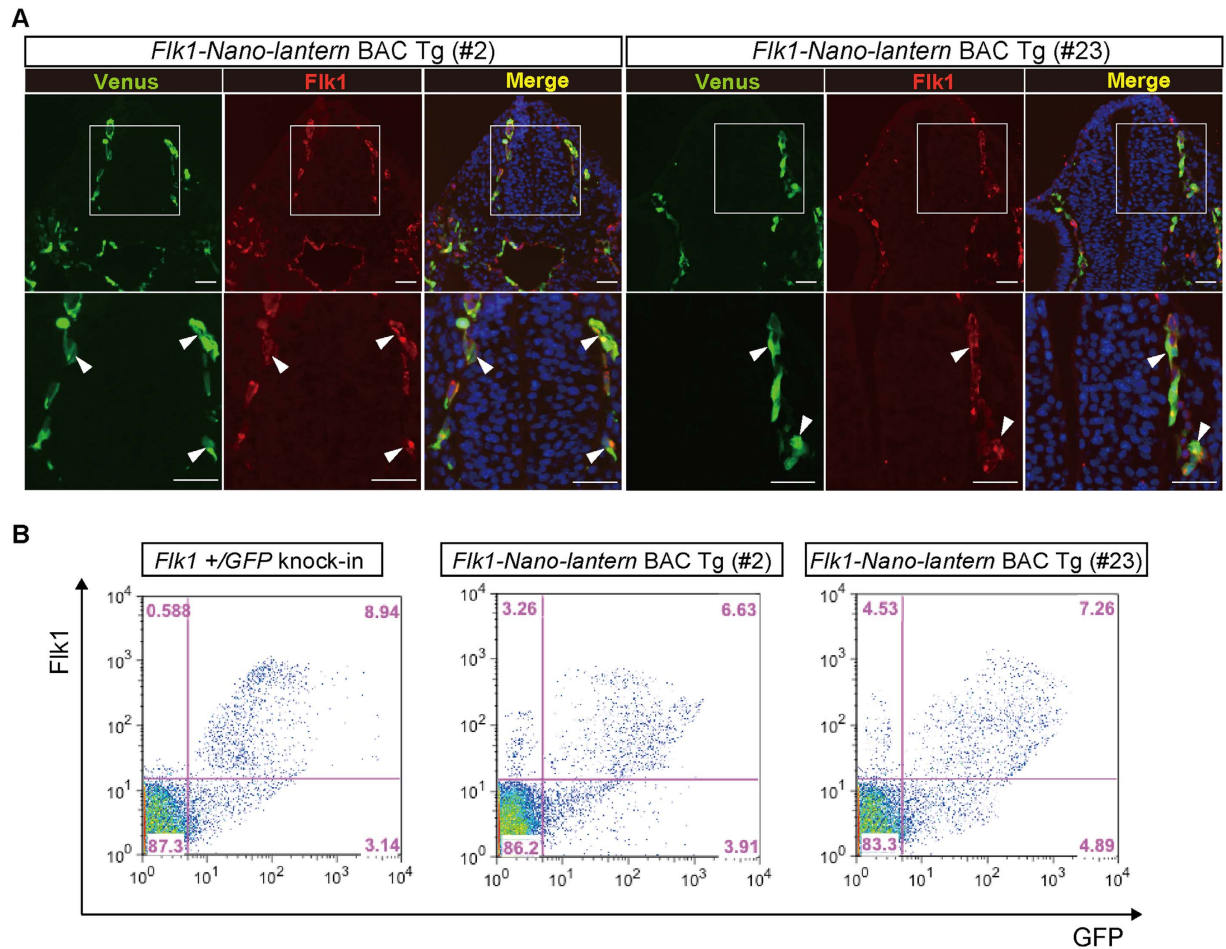


Figure 3. Faithful expression of *Nano-lantern* driven by the *Flk1* regulatory sequence in vascular ECs. Venus expression in *Flk1-Nano-lantern* BAC Tg embryos at 9.5 dpc. (A) Co-expression of Venus and the endogenous Flk1 protein. Transverse sections posterior to the heart of *Flk1-Nano-lantern* BAC Tg embryos (#2 and #23) were subjected to immunohistochemical analysis with anti-GFP and anti-Flk1 antibodies to further compare the distribution of their expression. Arrowheads indicate ECs with co-expression of Venus and Flk1. Scale bars: 50 μ m. (B) Flow cytometric analysis of *Flk1-Nano-lantern* BAC Tg embryos at 9.5 dpc (#2 and #23). Single cells prepared from *Flk1-Nano-lantern* BAC Tg embryos was incubated with PE-labelled anti-Flk1 antibody and flow cytometry was performed as described in Materials and Methods.

BAC Tg mice also recapitulated *Flk1* expression in tumour ECs. Previously, Kappel and colleagues identified enhancer activity in the first intron of the *Flk1* gene to direct *Flk1* expression in ECs during development³¹. This enhancer was successfully used to drive mCherry expression in ECs by other researchers. However, deletion of this enhancer has no significant effect on *Flk1* expression in ECs at 9.5 days post-coitus (dpc) or mesodermal progenitors at 7.5 dpc²⁵. These results suggest that an unidentified enhancer directs *Flk1* expression in ECs and mesodermal cells. BAC Tg mice and a comparative genome approach showed that the DMME (distal multipotent mesoderm enhancer) located 15 kb upstream of the *Flk1* gene directs Flk1 expression in mesodermal cells during gastrulation and in neural cells of the retina^{21–29}. Therefore, the *Flk1-Nano-lantern* BAC Tg mice generated in this study will be useful for recapitulating endogenous *Flk1* expression in ECs as well as neural and mesodermal cells during development.

Flk1 was expressed not only in vascular ECs but also in lymphatic ECs, which regulates lymphatic vessel sprouting by forming heterodimers with Flt4³². Albuquerque and colleagues reported that a splice variant of the gene encoding Flk1, which was called soluble Flk1 (sFlk1), regulates lymphangiogenesis by blocking VEGF-C functions²⁶. sFlk1 enhances corneal allograft survival and suppresses lymphangioma cell proliferation. These results indicate that sFlk1 might become a therapeutic agent for lymphatic diseases such as lymphatic vascular malformations and tumour lymphangiogenesis. Because our *Flk1-Nano-lantern* BAC Tg mice recapitulate lymphatic Flk1 expression, they would be useful for visualizing *Flk1* expression non-invasively during lymphangiogenesis associated with human diseases.

Nano-lantern-expressing cells have been clearly visualized by their bioluminescence [18]. Consistent with that previous report, a bright bioluminescence was detected in ECs of the aortic rings from *Flk1-Nano-lantern*

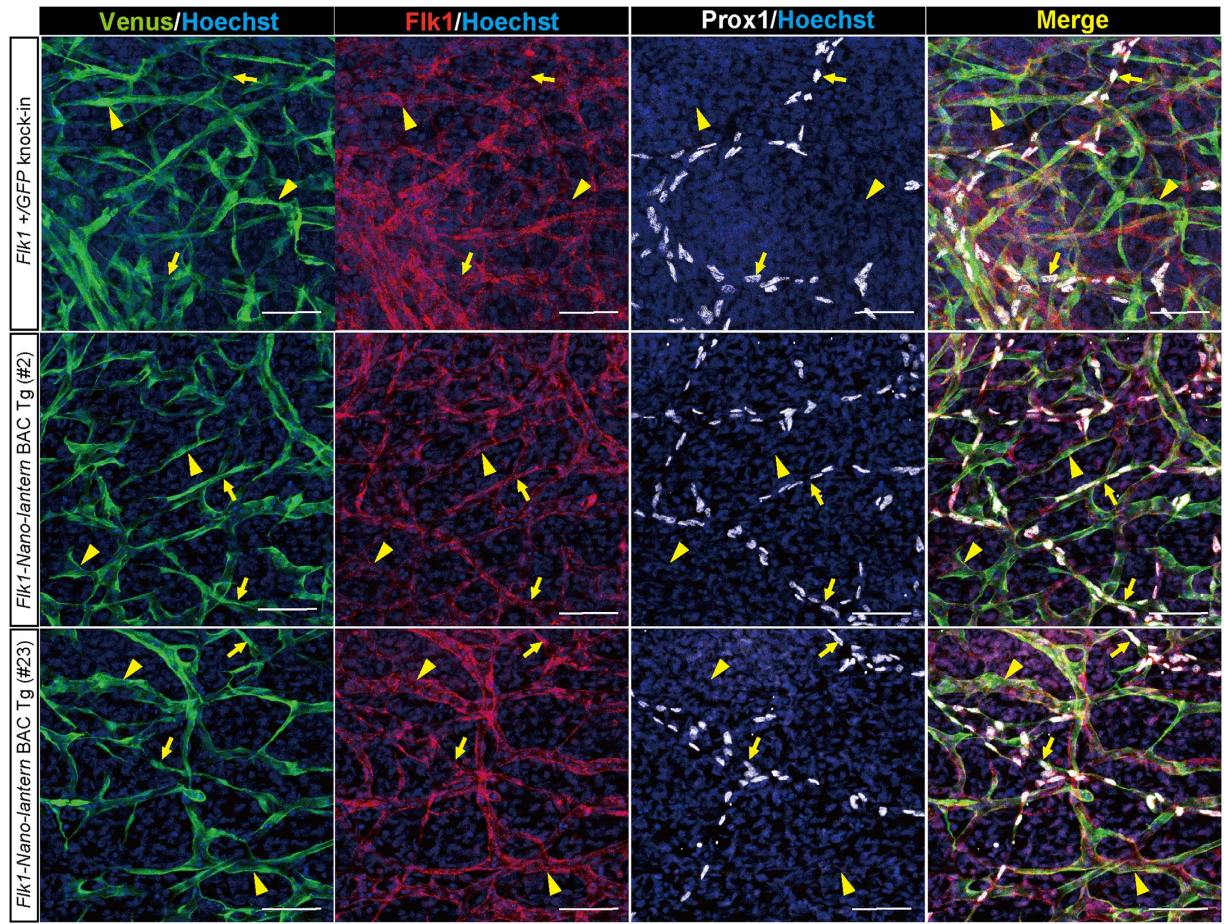


Figure 4. Expression of *Flk1-Nano-lantern* in lymphatic ECs. Immunohistochemical analysis of the back skin of *Flk1-Nano-lantern* BAC Tg mice with anti-GFP, -Flk1 and -Prox1 antibodies. Arrows and arrowheads indicate Prox1-positive lymphatic ECs and Prox1-negative vascular ECs, respectively. Scale bars: 50 μ m

BAC Tg mice, and time-lapse imaging of EC sprouting over 18 hr was achieved without phototoxicity (Fig. 6, Supplementary Movie S1), showing a clear advantage over *Flk1-GFP* BAC Tg mice.

Flk1 is a major mediator of tumour angiogenesis. Therefore, targeting its pathway has been considered an integral component of cancer treatment. Bevacizumab (Avastin), a humanized anti-VEGF antibody, was the first angiogenic inhibitor for cancer patients¹⁵. Sunitinib (Sutent) inhibits platelet-derived growth factor receptors and VEGF receptors as a multiple receptor tyrosine kinase inhibitor, which was approved by the U.S. Food and Drug Administration for the treatment of renal cell carcinoma and imatinib-resistant gastrointestinal stromal tumours³³. The multikinase inhibitor sorafenib (Nexavar) is considered a useful drug for the treatment of renal cancer and hepatocellular carcinoma^{34,35}. Because we have shown that *Flk1-Nano-lantern* BAC Tg mice can be used for bioluminescence imaging of tumour vessels even in freely moving mice, the detection sensitivity for the bioluminescence is very high and this Tg mouse line would be applicable for screening anti-tumour angiogenesis drugs.

Materials and Methods

Construction of the *Flk1-Nano-lantern* BAC transgene. A BAC clone (RP24-125B24) encompassing the *Flk1* locus was modified using the RED/ET recombination method (Gene Bridges, Heidelberg, Germany)²⁰. A DNA fragment encoding *Nano-lantern-SV40 polyA*¹⁹ was ligated to a DNA fragment encoding an FRT PGK-gb2 neo expression cassette that comprises a prokaryotic promoter and neomycin-resistance gene flanked by FRT sequences (Gene Bridges). Homology arms for the first exon of *Flk1* were amplified by two pairs of primers as follows: 5'arm-1: 5'-cgaagagagtctcacttgaggc-3', 5'arm-2: 5'-ggcacagactggttccctcctg-3', 3'arm-1: 5'-catcgttgagcgtgtcctcggag-3', and 3'arm-2: 5'-gagtatttagttaatacacctgg-3'. Then, the arms were ligated to both ends of the reporter cassette. The neo cassette was excised by inducing FLPe expression after introduction of the FLPe expression plasmid (Gene Bridges). Recombination of BAC clones was confirmed by PCR analysis. *Flk1-Nano-lantern* BAC DNA was prepared using a Nucleobond Xtra BAC column (Macherey-Nagel, Düren, Germany) and then linearized by *PI-SceI* digestion. The BAC DNA was then subjected to pulse field electrophoresis.

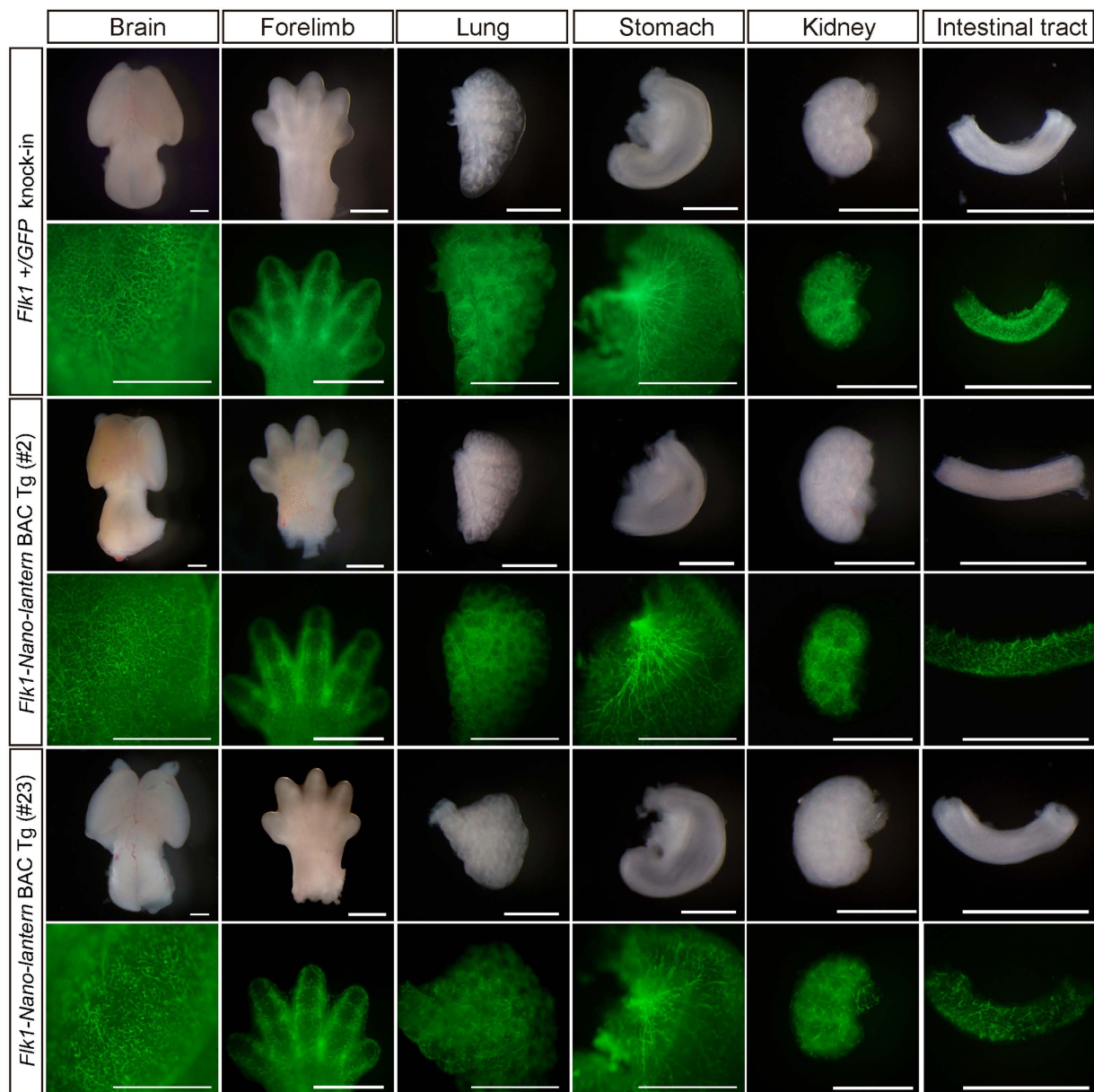


Figure 5. Expression of Venus in various organs from *Flk1*-Nano-lantern BAC Tg mice. Organs from *Flk1*+/*GFP* mice and *Flk1*-Nano-lantern BAC Tg mice (#2 and #23) were dissected out and subjected to imaging with a Leica FLIII. Scale bars: 1 mm.

Mice. Experimental procedures were approved by the Animal Care and Use Committee of Shiga University of Medical Science and methods were carried out in accordance with the approved guideline (Approval number: 13-105). *Flk1*-Nano-lantern BAC Tg DNA was injected into the pronuclei of fertilized eggs collected from C57BL/6J females. The injected eggs were transplanted into pseudo-pregnant ICR females (SLC Inc., Shizuoka, Japan). *Flk1*-Nano-lantern BAC Tg animals were maintained by mating with C57BL/6J mice and genotyped by PCR using the following primers: GFP-S: 5'-AGCAAGGGCGAGGAGCTGTTTACC-3' and GFP-AS: 5'-TGCCGTCGTCCTTGAAGAAGATG-3'. Fluorescent signals in the skin and ears were used to discriminate *Flk1*-Nano-lantern BAC Tg and wild-type (WT) mice. Fluorescence images of postnatal mice were taken by a Nikon D3300 camera with an AF-S DX NIKKOR 18-55 mm f/3.5-5.6 G VR II lens (Nikon, Tokyo, Japan). A filter (Marumi Cross Screen, Tokyo, Japan) was used to detect GFP fluorescence under an Ex FlashLight ExF-MxB (BioTools, Jupiter, FL, USA). For the detection of bioluminescence, *Flk1*-Nano-lantern BAC Tg animals on a C57BL/6J background were back-crossed by mating with B6 (Cg)-*Tyr*^{c-2J} mice (The Jackson Laboratory, Bar Harbor, ME, USA).

Immunohistochemistry. Embryos and tumours were dissected in cold PBS, fixed in 4% paraformaldehyde overnight, and mounted in OCT (Surgipath FSC 22 Blue Frozen section compound; Leica, Wetzlar, Germany) as

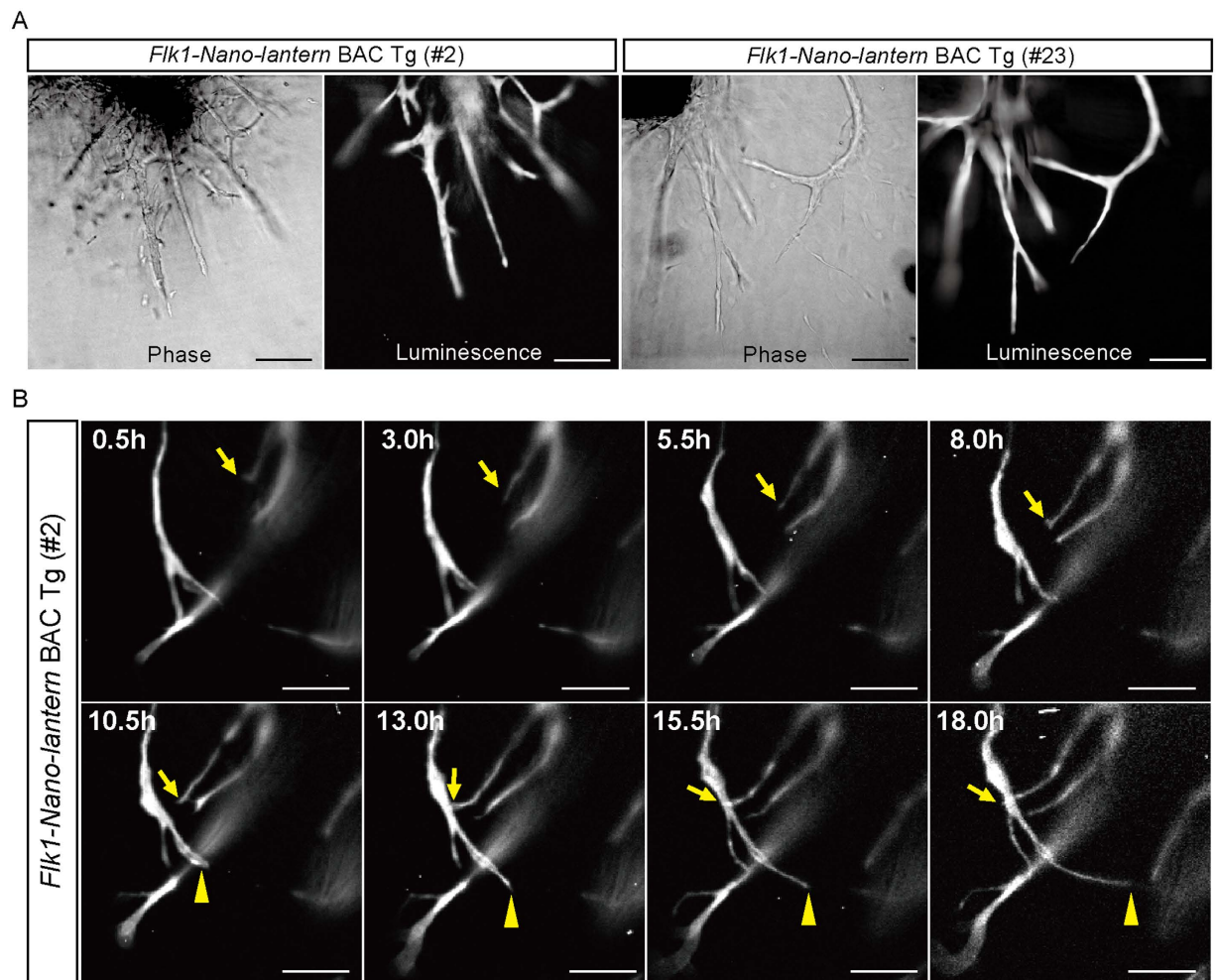


Figure 6. Luminescence imaging of ECs in aortic ECs of *Flk1-Nano-lantern* BAC Tg mice. (A) Detection of luminescence in endothelial cells in the aortic rings from *Flk1*+/*GFP* mice and *Flk1-Nano-lantern* BAC Tg mice. The aortic rings were isolated from *Flk1*+/*GFP* mice and *Flk1-Nano-lantern* BAC Tg mice (#2 and #23) and cultured in the presence of VEGF-A. Luminescence was detected after the addition of coelenterazine-h to the media. Scale bars: 100 μ m. (B) Time-lapse luminescence imaging of sprouting ECs. Luminescence was detected every 30 min and recorded over an 18 hr period. Arrows and arrowheads indicate sprouting ECs. Scale bars: 10 μ m.

described previously³⁶. Tissue blocks were sectioned using a cryostat (CM1860 UV; Leica). The sections from the embryos were incubated with a rat monoclonal antibody against mouse *Flk1* (clone AVAS12, BD Pharmingen, Franklin Lakes, NJ, USA) and an Alexa Fluor 488-conjugated rabbit polyclonal anti-GFP antibody (A21311; Life Technology, Carlsbad, CA, USA) overnight at 4 °C. Bound primary antibodies were detected with secondary Cy5-conjugated donkey anti-rat IgG (712-175-153; Jackson Immuno Research, West Grove, PA, USA). The sections from the LLC tumours were incubated with a rabbit monoclonal antibody against mouse *Flk1* (clone 55B11, Cell Signaling, Danvers, MA, USA) and subsequently Alexa Fluor 594-conjugated donkey polyclonal anti-rabbit IgG antibody (Life Technology). Then, Alexa Fluor 488-conjugated rabbit polyclonal anti-GFP antibody (Life Technology) was used to detect GFP overnight at 4 °C. Nuclei were stained with 5 g/ml Hoechst 33342 (Invitrogen, Carlsbad, CA, USA).

Whole mount immunohistochemistry on the embryos was performed as described previously²¹. Embryos were dissected and fixed in 4% paraformaldehyde overnight. After washing with PBS, the embryos were treated with a blocking solution (2% dry skim milk and 0.1% Tween 20 in PBS) for 1 hr and then incubated with primary antibodies at 4 °C overnight. The embryos were washed in PBST for 5 min twice and then incubated with fluorochrome-conjugated secondary antibodies at room temperature for 1 hr. Nuclei were visualized by incubation with 2 μ g/ml Hoechst 33342 for 10 min at room temperature. For the visualization of skin lymphatic endothelial cells, we followed the protocol by James *et al.*³⁷. We used goat anti-Prox1 antibody (AF2727, R&D systems, Minneapolis, MN, USA).

Confocal microscopy. Images of embryos were captured by a BioRevo inverted microscope with a GFP-B filter (Keyence Osaka, Japan) or Leica MZ FLIII with a GFP LP filter (Leica, Wetzlar, Germany). Confocal images

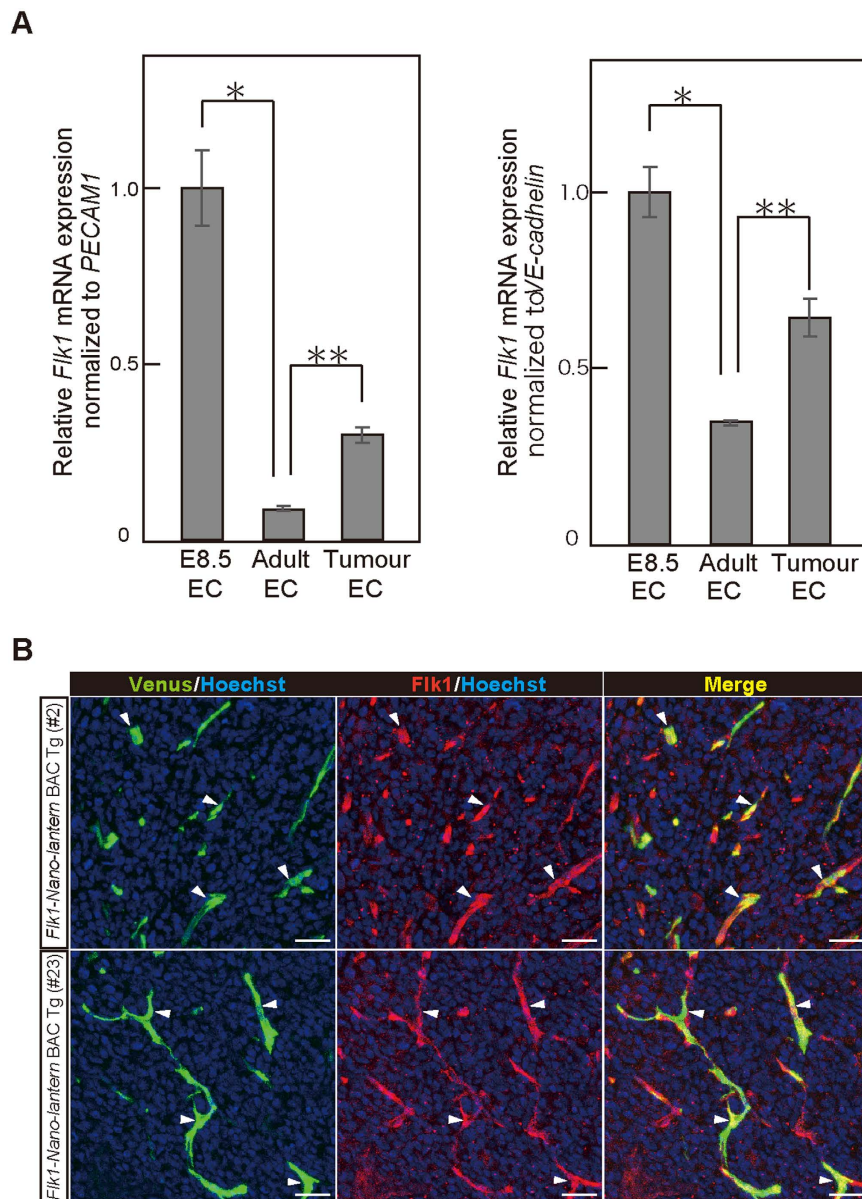


Figure 7. Bioluminescence imaging of tumour blood vessels in *Flk1-Nano-lantern* BAC Tg mice. Relative *Flk1* gene expressions in ECs from embryos at E8.5 (E8.5 EC), adult skin (A) Adult EC, and LLC tumours (Tumour EC) normalized by PECAM1 (platelet endothelial cell adhesion molecule-1) (left) and VE-cadherin (right). (B) Immunohistochemical analysis of LLC tumours in *Flk1-Nano-lantern* BAC Tg mice (#2 and #23) with anti-*Flk1* and anti-GFP antibodies. Arrowheads indicate ECs with co-expression of Venus and *Flk1*. Scale bars: 100 μ m. LLC cells were implanted into the backs of *Flk1-Nano-lantern* BAC Tg mice and maintained for 8 days.

were acquired on a Leica TCS-SP8 (Leica). Embryos were mounted in 80% glycerol on glass-bottom dishes (IWAKI, Tokyo, Japan). Fluorescence was excited with a 405-nm UV laser for Hoechst 33342, a 638-nm laser for Cy5 or Alexa Fluor 633, a 552-nm laser for Cy3, and a 488-nm laser for Alexa Fluor 488. A hybrid detector was used for signal amplification.

Aortic ring assay. The aortic ring assay was performed as described previously²². Briefly, thoracic aortae were excised from *Flk1-Nano-lantern* BAC Tg mice, and peri-aortic tissues, such as the fat layer and adventitia, were removed using fine microdissecting forceps and iridectomy scissors. Rings of approximately 1 mm in length were prepared in serum-free Dulbecco's modified Eagle's medium (DMEM) (Sigma, St. Louis, MO, USA). Individual rings were embedded in type I collagen gel (Nitta Gelatin, Osaka, Japan) on glass-bottom dishes and cultured in DMEM containing 50 ng/ml human recombinant VEGF-A (R&D systems). After 1 week of culture at 37 °C in a humidified environment, the collagen gels containing the aortic rings were fixed in 4% paraformaldehyde for 30 min.

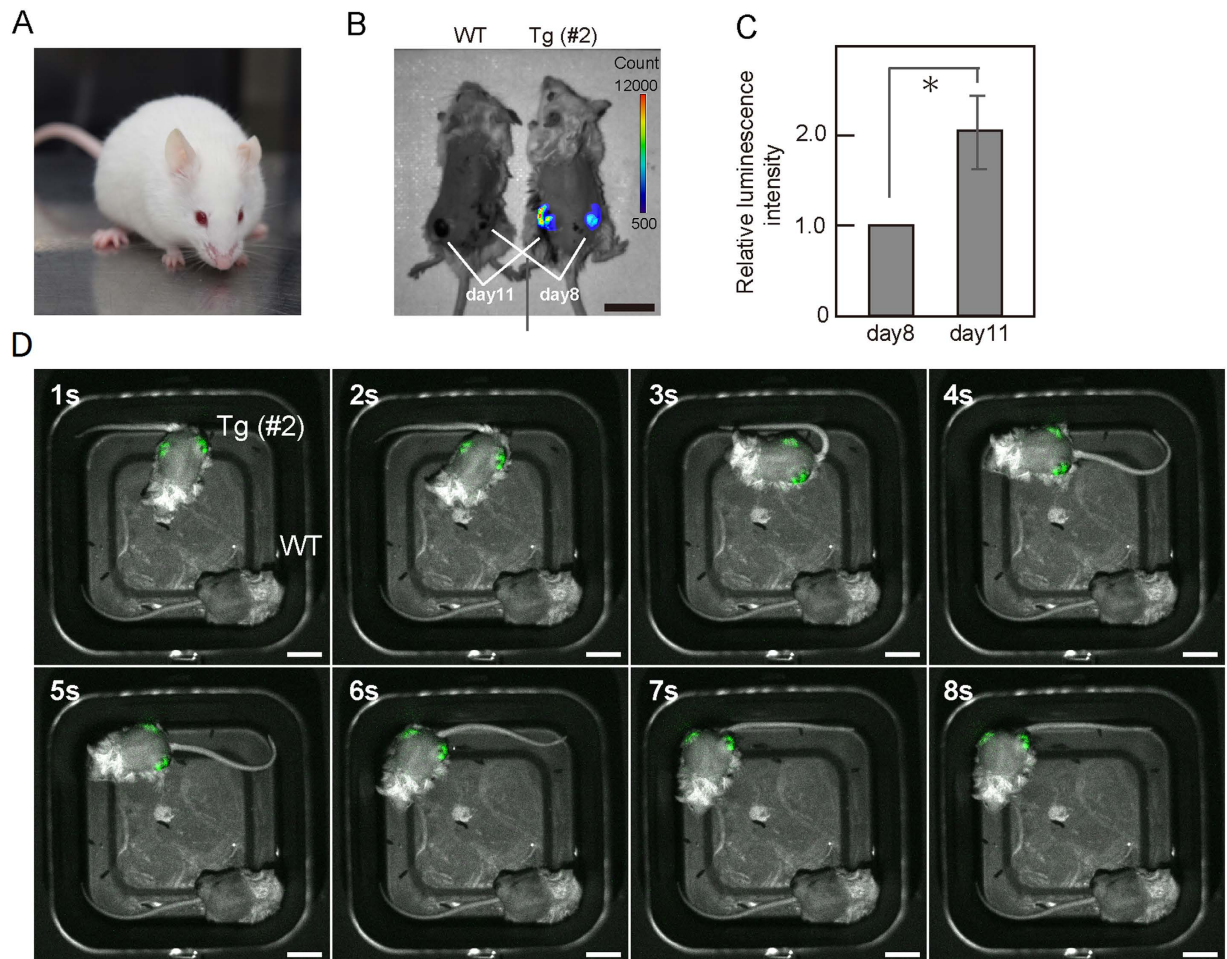


Figure 8. Bioluminescence imaging of tumour ECs in *Flk1-Nano-lantern* BAC Tg mice. (A) Coat colour of *Flk1-Nano-lantern* BAC Tg:: B6 (Cg)-Tyr^{c-2l} mice. (B) Representative luminescence image of *Flk1-Nano-lantern* BAC Tg mice (#2) with LLC tumours (day 8 and day 11) at 30 s exposure. Scale bar, 2 cm. (C) Relative luminescence intensity of the tumours. Luminescence from the tumours on day 8 and day 11 was measured, and the relative value of the luminescence of the tumour on day 11 to that on day 8 was calculated. Asterisks indicate statistical significance. * $P < 0.05$. (D) Consecutive frames of video-rate luminescence images of *Flk1-Nano-lantern* BAC mice with LLC tumours. The luminescence signal every 1 s is shown in green. Scale bar, 2 cm.

Luminescence imaging of aortic ring assay. For luminescence imaging, 5 mM coelenterazine-h (Wako, Osaka, Japan) dissolved in EtOH was added to 2 ml of the medium (final concentration of 5 μ M) in a glass-bottom dish. Half of the imaging media was replaced with media containing 5 μ M coelenterazine-h every 6 hr. A LV200 inverted microscope with a 20 \times , NA 0.70, UCPlanFLN objective (Olympus, Tokyo, Japan) was used for the aortic ring assay. Luminescence was recorded by an Imagem \times 2 EMCCD camera (Hamamatsu, Shizuoka, Japan) without an emission filter every 30 min.

Reverse-transcription (RT)-qPCR analysis. Total RNA was extracted using an RNeasy Mini kit (Qiagen, Hilden, Germany). For RT-qPCR analysis, first-strand cDNA was synthesized from total RNA using a QuantiTect Reverse Transcription kit (Qiagen). qPCR was performed with SYBR Premix Ex Taq II (Takara, Shiga, Japan) on a Thermal Cycler Dice Real Time System (TP850; Takara). The amount of target RNA was estimated using an appropriate standard curve and divided by the estimated amount of β -actin mRNA.

Tumour implantation. Lewis lung carcinoma (LLC) cells were cultured in DMEM containing 10% foetal bovine serum (Sigma). After the LLC cells were trypsinized, 1×10^6 cells were suspended in D-PBS(-) (Nacalai Tesque, Kyoto, Japan) and implanted into the back of a mouse. To examine tumour angiogenesis, we implanted LLC cells in 12-week-old WT and *Flk1-Nano-lantern* BAC Tg mice.

Isolation of tumour ECs from mice. ECs from the skin or tumours in mice were isolated as previously described³⁸. In brief, tumour or skin tissues were finely minced after resection and digested with dispase II (Godo Shusei, Chiba, Japan), collagenase type I (Wako, Osaka, Japan), and collagenase type II (Worthington Biochemical Corp., Lakewood, NJ, USA) in a 50-ml tube. The digested tissue was passed through 40- μ m filters to yield single

cell suspensions. Fluorescence-labelled anti-CD45 and -CD31 mAbs (BD Biosciences, San Jose, CA, USA) were used. CD31 + CD45-ECs were sorted by using a SORP FACSria (BD Biosciences).

Bioluminescence imaging of tumour angiogenesis. Video-rate imaging of freely moving *Flk1-Nano-lantern* BAC Tg:: B6 (Cg)-Tyr^{c-2j} mice and WT B6 (Cg)-Tyr^{c-2j} mice was performed as described previously¹⁹. Briefly, 8 g of coelenterazine-h (12 µl EtOH + 48 µl D-PBS(-); final volume 60 µl) was injected inside the LLC tumour using an insulin syringe with a 23 G needle followed by imaging after 1 min. For video-rate observation, we used a Lumazone *in vivo* luminescence imaging system (Molecular Devices, California, USA) equipped with an Evolve512 EMCCD camera (Photometrics, Arizona, USA) and a HF12.5SA-1 lens (Fujifilm, Tokyo, Japan). Bright field images under illumination by a LightEngine SPECTRA (Lumencor, Oregon, USA) and luminescence images taken in the dark were captured alternatively. To adjust the timing of the light illumination, pulsed signals for turning on the light were generated by a WF1973 multifunction generator (NF Corporation, Yokohama, Japan) according to exposure time-out signals from the EMCCD camera.

Flow cytometry. Flow cytometric analysis was performed as described previously. Fluorescent dye-labelled anti-Flk1 (BD Biosciences, San Jose, CA, USA, clone AVAS12) was used to stain the cells. Stained cells were analysed with a FACSCalibur (BD Biosciences). Data were analysed by FlowJo software (TreeStar, Ashland, OR, USA).

Statistical analysis. Student's *t* tests were used to assess the level of significance between groups.

References

- Gerhardt, H. *et al.* VEGF guides angiogenic sprouting utilizing endothelial tip cell filopodia. *J Cell Biol.* **161**, 1163–1177 (2003).
- Mazzone, M. *et al.* Heterozygous deficiency of PHD2 restores tumour oxygenation and inhibits metastasis via endothelial normalization. *Cell* **136**, 839–851 (2009).
- Folkman, J. Tumour angiogenesis: therapeutic implications. *N. Engl. J. Med.* **285**, 1182–1186 (1971).
- Ferrara, N., Gerber, H. P. & LeCouter, J. The biology of VEGF and its receptors. *Nat. Med.* **9**, 669–676 (2003).
- Ferrara, N. & Kerbel, R. S. Angiogenesis as a therapeutic target. *Nature* **438**, 967–974 (2005).
- Endrich, B., Reinhold, H. S., Gross, J. F. & Intaglietta, M. Tissue perfusion inhomogeneity during early tumor growth in rats. *J. Natl. Cancer Inst.* **62**, 387–395 (1979).
- Carmeliet, P. & Jain, R. K. Principles and mechanisms of vessel normalization for cancer and other angiogenic diseases. *Nat. Rev. Drug Discov.* **10**, 417–427 (2011).
- Jain, R. K. Normalization of tumor vasculature: An emerging concept in antiangiogenic therapy. *Science* **307**, 58–62 (2005).
- Goel, S. *et al.* Normalization of the vasculature for treatment of cancer and other disease. *Physiol Rev.* **91**, 1071–1121 (2011).
- Leite de Oliveira, R. *et al.* Gene-targeting of Phd2 improves tumor response to chemotherapy and prevents side-toxicity. *Cancer Cell* **22**, 263–277 (2012).
- Ghajar, C. M. *et al.* The perivascular niche regulates breast tumour dormancy. *Nat. Cell Biol.* **15**, 807–817 (2013).
- Coults, L., Chawengsaksophak, K. & Rossant, J. Endothelial cells and VEGF in vascular development. *Nature* **438**, 937–945 (2005).
- Shibuya, M. Structure and dual function of vascular endothelial growth factor receptor-1 (Flt-1). *Int. J. Biochem. Cell Biol.* **33**, 409–420 (2001).
- Blanco, R. & Gerhardt, H. VEGF and Notch in tip and stalk cell selection. *Cold Spring Harb. Perspect. Med.* **3**, a006569 (2013).
- Hurwitz, H. *et al.* Bevacizumab plus irinotecan, fluorouracil, and leucovorin for metastatic colorectal cancer. *N. Engl. J. Med.* **350**, 2335–2342 (2004).
- Miller, K. *et al.* Paclitaxel plus bevacizumab versus paclitaxel alone for metastatic breast cancer. *N. Engl. J. Med.* **357**, 2666–2676 (2007).
- Welti, J., Loges, S., Dimmeler, S. & Carmeliet, P. Recent molecular discoveries in angiogenesis and antiangiogenic therapies in cancer. *J. Clin. Invest.* **123**, 3190–3200 (2013).
- Ebos, J. M. & Kerbel, R. S. Antiangiogenic therapy: impact on invasion, disease progression, and metastasis. *Nat Rev Clin Oncol.* **8**, 210–221 (2011).
- Saito, K. *et al.* Luminescent proteins for high-speed single-cell and whole-body imaging. *Nat. Commun.* **3**, 1262 (2012).
- Ishitobi, H. *et al.* Flk1-GFP BAC Tg mice: an animal model for the study of blood vessel development. *Exp. Animals* **59**, 615–622 (2010).
- Ishitobi, H. *et al.* Molecular basis for Flk1 expression in hemato-cardiovascular progenitors in the mouse. *Development* **138**, 5357–5368 (2011).
- Matsumoto, K. *et al.* Study of normal and pathological blood vessel morphogenesis in Flt1-tdsRed BAC Tg mice. *Genesis* **50**, 561–571 (2012).
- Ema, M., Takahashi, S. & Rossant, J. Deletion of the selection cassette, but not cis-acting elements, in targeted Flk1-lacZ allele reveals Flk1 expression in multipotent mesodermal progenitors. *Blood* **107**, 111–117 (2006).
- Kojima, T. *et al.* Subventricular zone-derived neural progenitor cells migrate along a blood vessel scaffold toward the post-stroke striatum. *Stem Cells* **28**, 545–554 (2010).
- Kubota, Y. *et al.* Isolation and function of tissue resident vascular precursors marked by myelin protein zero. *J. Exp. Med.* **208**, 949–960 (2011).
- Albuquerque, R. J. *et al.* Alternatively spliced vascular endothelial growth factor receptor-2 is an essential endogenous inhibitor of lymphatic vessel growth. *Nat. Med.* **15**, 1023–1030 (2009).
- Baker, M. *et al.* Use of the mouse aortic ring assay to study angiogenesis. *Nat. Protoc.* **7**, 89–104 (2011).
- Shalaby, F. *et al.* Failure of blood-island formation and vasculogenesis in Flk1-1-deficient mice. *Nature* **376**, 62–66 (1995).
- Okabe, K. *et al.* Neurons limit angiogenesis by titrating VEGF in retina. *Cell* **159**, 584–596 (2014).
- Shibuya, M. & Claesson-Welsh, L. Signal transduction by VEGF receptors in regulation of angiogenesis and lymphangiogenesis. *Exp. cell Res.* **312**, 549–560 (2006).
- Kappel, A. *et al.* Identification of vascular endothelial growth factor (VEGF) receptor-2 (Flk-1) promoter/enhancer sequences sufficient for angioblast and endothelial cell-specific transcription in transgenic mice. *Blood* **93**, 4284–4292 (1999).
- Veikkola, T. *et al.* Signalling via vascular endothelial growth factor-3 is sufficient for lymphangiogenesis in transgenic mice. *EMBO J.* **20**, 1223–1231 (2001).
- Faivre, S. *et al.* Safety, pharmacokinetic, and antitumor activity of SU11248, a novel oral multitarget tyrosine inhibitor, in patient with cancer. *J. Clin. Oncol.* **24**, 25–35 (2006).
- Escudier, B. *et al.* Sorafenib in advanced clear-cell renal-cell carcinoma. *N. Engl. J. Med.* **356**, 125–134 (2007).
- Llovet, J. M. *et al.* Sorafenib in advanced hepatocellular carcinoma. *N. Engl. J. Med.* **359**, 378–390 (2008).

36. Ema, M. *et al.* Primitive erythropoiesis from mesodermal precursors expressing VE-cadherin, PECAM-1, Tie2, endoglin, and CD34 in the mouse embryo. *Blood* **108**, 4018–4024 (2006).
37. James, J. M., Nalbandian, A. & Mukoyama, Y. S. TGF β signaling is required for sprouting lymphangiogenesis during lymphatic network development in the skin. *Development* **140**, 3903–3914 (2013).
38. Naito, H. *et al.* Identification and characterization of a resident vascular stem/ progenitor cell population in preexisting blood vessels. *EMBO J.* **31**, 842–855 (2012).

Acknowledgements

We would like to thank Ms. Yuko Hamada for her helpful assistance. This work was supported in part by a grant from PRESTO, Japan Science and Technology Agency (JST) (to M.E.), JSPS KAKENHI Grant number 26290030 (to M.E.) and “JST-SENTAN” and the MEXT Scientific Research on Innovative Areas, ‘Spying minority in biological phenomena’ (No. 3306) to T. Nagai. We also thank the Bionanophotonics Consortium (BNPC) for assistance in experiments using microscopy.

Author Contributions

J.M., C.W. and K.M. performed immunohistochemistry and FACS. S.I. performed luminescence imaging of the aortic rings. T. Nishie. and J. T. designed and constructed the BAC vector. S.I., T. Nagai, T.S., K.M., and Y.M. performed bioluminescence imaging of the tumours. K.M. assisted with the aortic ring assays and co-wrote the paper. K.T., H.N., H.K., and N.T. prepared endothelial cells from normal tissues and tumours. T. Nagai. provided essential materials. S.T. established the transgenic mice. M.E. designed the study and wrote the paper.

Additional Information

Supplementary information accompanies this paper at <http://www.nature.com/srep>

Competing Interests: The authors declare no competing financial interests.

How to cite this article: Matsushita, J. *et al.* Fluorescence and Bioluminescence Imaging of Angiogenesis in *Flk1-Nano-lantern* Transgenic Mice. *Sci. Rep.* **7**, 46597; doi: 10.1038/srep46597 (2017).

Publisher's note: Springer Nature remains neutral with regard to jurisdictional claims in published maps and institutional affiliations.



This work is licensed under a Creative Commons Attribution 4.0 International License. The images or other third party material in this article are included in the article's Creative Commons license, unless indicated otherwise in the credit line; if the material is not included under the Creative Commons license, users will need to obtain permission from the license holder to reproduce the material. To view a copy of this license, visit <http://creativecommons.org/licenses/by/4.0/>

© The Author(s) 2017